Ammonia gas mitigation by reactive absorption

Vitor Moritz Moser [1], Marcela Kotsuka da Silva [1], Jaci Carlo Schramm Câmara Bastos [1*]

[1] *Departamento de Engenharia Química, Universidade Regional de Blumenau, 89030-000 Blumenau, Santa Catarina, Brazil*
** Corresponding author. E-mail: jcscbastos@furb.br*

ABSTRACT. Odors from the decomposition of organic matter in rendering plants, bioenergy facilities, and composting plants cause notable environmental and health impacts in nearby communities due to the significant emission of ammonia gas, making the implementation of mitigation technologies essential. This study aimed to evaluate a pilot-scale reactive absorption column for treating a concentrated stream of ammonia gas and to simulate industrial-scale equipment. A coupled experimental and numerical investigation was conducted; a pilot-scale chemical scrubber was set up, and a 3^2 experimental design were performed with concentrations of ammonia and sulfuric acid as factors. The results demonstrated effective treatment with removal rates varying from 6.3% to 44.9%, with the limiting factor being the acid concentration in the scrubbing solution. Data were analysed using surface response methodology, and coupled numerical models were employed to determine the mass transfer coefficient and reaction rate constant. These data were regressed numerically and fitted into a microscopic mathematical model that accounted for both gas absorption by the liquid and the chemical reactions; this approach enabled the estimation of key parameters such as specific reaction rates and mass transfer. Finally, numerical studies were carried out to assess industrial-scale behaviour, explore scenarios for scale-up, predict equipment dimensions, and confirm the feasibility of industrial application. Results indicated that the industrial reactive absorption column could treat an ammonia stream flowing at approximately 27,000 m^3/h (7.97kg/m^3 of NH_3) with near 100% efficiency.

Key words: pilot and industrial scale; scrubber; numerical simulation; parameter regression; pollutant emission

DOI: https://doi.org/10.33837/msj.v8i1.1738

Received: 12/09/2025 *Online Published: 19/11/2025*
Associate editor: Herbert J. Dias

INTRODUCTION

Scrubbers (absorption columns) are equipment widely discussed in literature, used industrially to treat air contaminated by pollutants generated in processes involving the decomposition of organic matter, as they help mitigate odors in the vicinity of critical environments. These technologies are reliable due to their effectiveness, achieving removal efficiencies of 98% for hydrogen sulphide (H_2S) and 99% for ammonia (NH_3) (Lebrero et al. 2013), or simultaneous treatment of both gases with a removal efficiency of 97%. In a more recent study, a chemical scrubber was used to treat SO_2 with ammonia, achieving 98% efficiency under maximum experimental performance conditions (Flagielo et. al 2025). An advantage over biological methods is that they lack the burden of not experiencing periods of performance decline, as the process's initialization does not depend on the growth of microorganisms. However, it has the disadvantage of increasing costs due to the consumption of chemicals, which can reach 69% of the technology's operating cost (Alinezhad et al. 2019). Although challenging, the overall process sustainability can be achieved by combining chemical absorption with other methods, for example, photolytic reactors, which have already demonstrated promising results in reducing chemical costs. (Prostejovsky et. al 2025).

Chemical scrubbers consist of a vertical chamber through which the air contaminant is transferred to a solution with a purifying function in a countercurrent flow, which is directed by mechanical ventilation from the emission source, sucking the contaminated air through ducts that centralize the demand. Such equipment is generally oversized to ensure effective removal during peak gas emission periods (Abdi et al. 2020). According to Yildirim et al. (2012), among the methods for mitigating chlorine gas release, absorption can be highlighted as the most important. Two mechanisms are typically involved: physical and chemical absorption; the first is applied when the gas phase is highly soluble in the liquid phase (Fthenakis, 2001) (e.g. NH_3 and HF) and only the interphase mass

transfer and the transport within each phase are important. In such processes, the system can be successfully characterized by means of the mass transfer coefficients and the operational conditions, such as pressure and temperature. On the other hand, when the solubility of the gas phase in the liquid phase is limited, chemical absorption is more appropriate. In this case, the interphase mass transfer mechanism also occurs, but an appropriate chemical reaction continuously removes the absorbed species in the liquid phase and, therefore, allows for greater transfer from the gas phase. Thus, in the reactive absorption process, besides the mass transfer coefficients and the operational conditions, the chemical reaction rate also plays a major role in the design, operation and optimization of the equipment. In this case, either the mass transfer rate or the chemical reaction rate can dominate the overall process. A balance of the relative importance between the mass transfer coefficient and the reaction rate constant is needed for the identification of the main mechanism.

In this study, a pilot-scale chemical scrubber was constructed to remove NH_3 from an H_2SO_4 solution, with the aim of reducing costs of the physical absorption process by the product formed from the chemical reaction. A methodology was developed to simultaneously study the mass transfer and chemical reaction phenomena in the liquid phase, through product quantitative analysis in samples collected at different equipment locations. Data processing was performed for subsequent regression in a mathematical model inherent to the reactive absorption process, i.e., they were statistically treated by surface response methodology to generate a polynomial function that can describe the system behaviour within the experimental range studied. Furthermore, the system was mathematically modelled, and the set of equations representing the material balance was solved using a numerical method. An inverse problem was then applied to predict the empirical parameters of the model, namely the mass transfer coefficient and reaction rate constant. Finally, a numerical simulation was carried out to assess the behaviour of the industrial-scale reactive absorption column. The methodology proposed allowed for the effective design of the equipment for a case of potential demand.

MATERIALS AND METHODS

Experimental Apparatus

The process dynamics investigation and evaluation of the physicochemical parameters were carried out in a pilot-scale reactive absorption column, schematized in Figure 1. The pilot system consists of a packed column with 116cm of height and 5cm of internal diameter; a 5L-balloon; CALLMEX® Model Q321A28 (690W) heating mantle, controlled by a potentiometer.

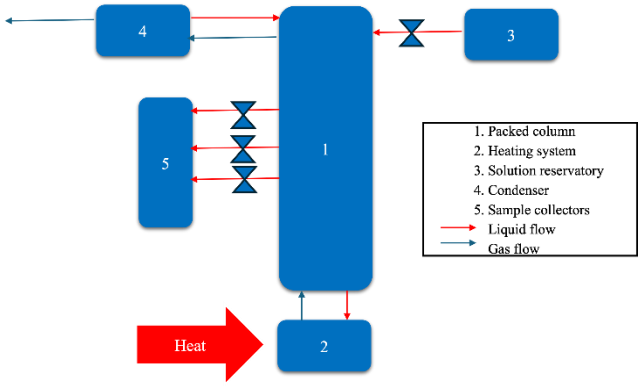

Figure 1. Experimental apparatus scheme.

An Allihn-type condenser was connected to the top; and the column was thermally insulated with glass wool and had three sampling outlets: 48, 64 and 80cm from the base. The column was filled with glass pellets, all cylindrical in shape and with an average size of 0.7cm and hollow inside, with diameters of approximately 0.5cm (external) and 0.2cm (internal) and a randomly arranged.

Experimental Test

The proposed procedure to simulate a chemical scrubber consists essentially of a test gas through the column in operation to collect samples along its length. For test safety, pure is not used to feed the process; instead, an ammonium hydroxide (NH_4OH) solution is prepared at a pre-planned concentration and placed in the flask. The heating system serves to shift the equilibrium of the solution toward converting ammonium ions into ammonia gas and forcing it through the column by steam stripping. For each experimental test, the following steps were followed in order: *a) Preparation of the apparatus:* clean the equipment with deionized water and check that the seals are completely closed. *b) Preparation of the ammonium hydroxide solution:* add 2L of deionized water to the flask and the expected volume of ammonium hydroxide. *c) Preparation of the purification solution:* in a 1000mL volumetric flask, a solution with the expected volume of sulfuric acid is prepared and then poured into the top reservoir. *d) Heating the column:* turn on the heating mantle at 80% power and monitor the

temperature until it reaches 100°C to start boiling. Once boiling begins, the water in the top condenser is turned on to maintain reflux. *e) Start of operation:* the purification solution inlet valve is opened at 8mL/min, and the timer starts. *f) Sample collection:* 18min after the operation starts, collection occurs at each of the three points. The column pressure itself pushes the liquid into the amber vial, thus each test produces three samples for analysis. After collecting the equipment is turned off. *g) Checking the liquid flow rate:* using a graduated cylinder, the remaining volume of the top solution (V_f) is measured. Equation 1 describes the liquid flow rate (Q_l) as a time function (t**).

$$Q_l = \frac{V_f - 1000mL}{t**} \quad (1)$$

h) Estimating steam flow rate: a combination of two equations is used. First, the one defining the liquid-vapor specific enthalpy (ΔH_{lv}) as the heat added to the system. Or, in temporal terms, the power added to the system (dq/dt) divided by the mass evaporated flow rate ($m = \frac{1}{H_{lv}}\frac{dq}{dt}$). Then, the mass flow rate is converted to volumetric using the specific mass of steam (ρ_v) as the ratio between the mass and volume of steam generated, or in this case, the ratio between the mass flow rate and the volumetric flow rate, as shown in Equation 2. Because the contaminant is highly diluted, the properties of water were used as a proxy for the system. For the heat addition rate term, 80% of the equipment's nominal power was assumed.

$$Q_g = \frac{1}{P_v \cdot \Delta H_{lv}} \cdot \frac{dq}{dt} \quad (2)$$

i) Estimation of ammonia concentration at the bottom inlet of the column: the total mass of ammonia entering the column is considered to be the product of the volume that passed through the pipette in step (b) (V_P), its specific mass (ρ_p), and its title - purity ratio in g/g (τ_P); while the total volume of evaporated liquid is the product of the vapor flow rate (Q_g) calculated in item *(h)* by the sample collection time (t*). Considering the hypothesis that the evaporation rate and ammonia concentration are constant over time, we have the following relationship (Equation 3).

$$C_{NH3(g)(entrada)} = \frac{m_p}{V_{l\to v}} = \frac{V_p \cdot p_p \cdot t_p}{Q_g \cdot t*} \quad (3)$$

j) Calculation of the acid concentration at the top of the column inlet: obtained directly from the relationship described in Equation 4.

$$C_{H2SO4\,(g)\,(entrada)} = \frac{V_p \cdot P_p}{1000mL} \quad (4)$$

Chemical Analysis

Kjeldahl analysis (Kjeldahl, 1983) is performed in triplicate to detect and quantify NH^{+}_{4} concentration (g/L) in each sample produced. In this method, 10mL was collected as the sample volume produced *(Va)* in the experimental test, and the test tube was filled with deionized water to 100mL; 1g of magnesium oxide (MgO) was added to a Macro Kjeldahl tube, and then 100mL of the solution was poured into it; the tube was immediately coupled to a nitrogen distiller (KJETEC SYSTEM 1002 Distilling Unit). In a 250mL Erlenmeyer, 15mL of nitrogen indicator solution (4% boric acid + methyl red: methylene blue 1:1) was placed into the condenser outlet of the nitrogen distiller. The equipment is turned on and begins producing vapor over the macro Kjeldahl tube. Shortly thereafter, condensate droplets are produced, which change the colour of the indicator solution from grey to green. The distillation lasted approximately 6 min, or enough time to produce 150mL of distillate. After, the distilled material was titrated with a standardized 0.1N sulfuric acid solution (Ca) with a correction factor *(Fc)*, Equation 5 expresses the result for ammonium ion concentration (C_{NH4+}).

$$C_{NH4+} = \frac{(Vt - Vb).Ca.Fc.14{,}007}{Va} \quad (5)$$

where Vt is the final volume of the sulfuric acid solution, and Vb the titrated blank sample volume.

Experimental Design

In this study, a 32 factorial design were applied, with concentration of $C_{NH3(g)(inlet)}$ and $C_{H2SO4(l)(inlet)}$ varying in 3 levels as shown in Table 1.

Table 1. Experiments carried out based on their variables

Experiment	$C_{H2SO4(l)(inlet)}$ (mL/L)	$C_{NH3(g)(inlet)}$ (mL/2L)
1	30 (-)	10.0 (+)
2	30 (-)	5.5 (0)
3	30 (-)	1.0 (-)
4	40 (0)	10.0 (+)
5	40 (0)	5.5 (0)
6	40 (0)	1.0 (-)
7	50 (+)	10.0 (+)
8	50 (+)	5.5 (0)
9	50 (+)	1.0 (-)

Surface Response Analysis

Using STATISTICA 7 ® software, the surface response of the removal percentage *(y)* was constructed as a function of the two variables. Equation 6 defines y

as the ratio between the product concentration at the liquid outlet and the pollutant demand concentration at the gas inlet (both points at z=0).

$$y = \frac{(C_{NH4+})\,l,z=0}{(C_{NH3})\,g,z=0} \quad (6)$$

Mathematical Model

The model is analogous to a similar study conducted by a research group at FURB to represent the passage and absorption of chlorine gas by an air purifier using a chemical reaction with sodium hydroxide (Soares et al. 2016). It consists of a system of four first-order ordinary differential equations with their respective boundary conditions, as denoted in Equations 7 to 12. It fundamentally considers the mass transfer phenomena of the pollutant from the gas phase to the liquid phase for subsequent chemical reactions in the liquid phase. The reaction kinetics were assumed to be pseudo-first-order, and double-film theory was used for mass transfer. Diffusive fluxes were neglected in comparison to convective fluxes, and variations were assumed to occur unidirectionally along the axial axis of the column (z-axis). The variations of four combinations of concentrations of chemical species in the system phases were evaluated: ammonia gas in the gaseous phase $(C_{NH3})g$, ammonia gas in the liquid phase $(C_{NH3})l$, sulfuric acid in the liquid phase $(C_{H2SO4})l$ and ammonium ions in the liquid phase $(C_{NH4+})l$. The equation also includes gas flow rate (Q_g), liquid flow rate (Q_l) and the cross-sectional area of the apparatus (A_{ST}).

a) *Conservation of ammonia mass in the gas phase where k_m is the mass transfer coefficient.*

$$\frac{d}{dz}(C_{NH3})_g = \frac{-k_m \cdot A_{st}}{Q_g}.\left[(C_{NH3})_g - (C_{NH3})_l\right] \quad (7)$$

b) Conservation of ammonia mass in the liquid phase

$$\frac{d}{dz}(C_{NH3})_l = \frac{A_{st}}{Q_l}.\left\{k_m \cdot \left[(C_{NH3})_g - (C_{NH3})_l\right] - k_r \cdot (C_{NH3})_l\right\} \quad (8)$$

c) Conservation of mass of ammonium ions in the liquid phase where k_r is the chemical reaction coefficient as k_r.

$$\frac{d}{dz}(C_{NH4+})_l = \frac{A_{st}}{Q_l}.k_r \cdot (C_{NH3})_L \quad (9)$$

d) Conservation of mass of sulfuric acid in the liquid phase

$$\frac{d}{dz}(C_{H2SO4})_l = \frac{A_{st}}{Q_l}.k_r \cdot (C_{NH3})_L \quad (10)$$

e) Boundary conditions at z=H (highest sample collection point)

$$\begin{aligned}(C_{H2SO4})_{l,z=H} &= (C_{H2SO4})_{(l)\,(entrada)}\\ (C_{NH3})_{l,z=H} &= 0\\ (C_{NH4+})_{l,z=H} &= 0\end{aligned} \quad (11)$$

e) Boundary conditions at z=0 (lowest sample collection point)

$$(C_{NH3})_{g,z=0} = (C_{NH3})_{(g)(entrada)} \quad (12)$$

Statistical Treatment

Data were processed from a first and second-order interaction perspective, calculating the effects of each variable conditioned on the system in the 3^2 design, as well as the combination of the two variables (Barros Neto et al., 2001). This generates a surface response, which serves as a proxy for the experimental data in the data regression. Data processed by the surface response relate to the percentage pollutant removal at the lowest point of the column, where the highest product concentration is expected.

Data regression to obtain k_m and k_r

Mathematical model, represented in Equations 7 to 12, was solved using the Runge-Kutta method, for obtaining the ammonia concentrations in both phases: ammonium ions and sulfuric acid. That is, the response of this system is always a set of four functions: $C_{NH3(g)(z)}$, $C_{NH3(l)(z)}$, $C_{NH4+(l)(z)}$ e $C_{H2SO4(l)(z)}$. All quantities related to the system, including those related to its geometry and the flow rates imposed on the process (A_{ST}, Q_l, Q_g), can be measured directly or indirectly, except for the global mass transfer constant (k_m) and the reaction constant (k_r). This study proposes obtaining an estimate of these via numerical regression of experimental data, using the Least Squares Method as the objective function. Therefore, it is necessary to point out that two matrices were used to solve this problem. One obtained from the experimental data $C_{NH4+exp}$ represented as a surface response. The other one, $C_{NH4+cal}$ is obtained from the model numerical solution using estimated k_m and k_r; Figure 4 presents the proposed algorithm. As described in Equation 13, the objective function promotes a routine of iterative calculations so that the square of the difference between both matrices is as small as possible, as illustrated in Figure 2.

$$\left[F_{obj}\right]_{\min} = \sum_{i=1}^{n}\left(C_{(NH4+)exp} - C_{(NH4+)cal}\right)^2 \quad (13)$$

It is important to emphasize that in this methodology, the experimental data are compared to the calibrated model data, but not directly. This data matrix is not represented by the direct results obtained from the experiments. Instead, the objective function compares the data virtually plotted by the surface

response, which represents the experimental matrix after appropriate statistical treatment.

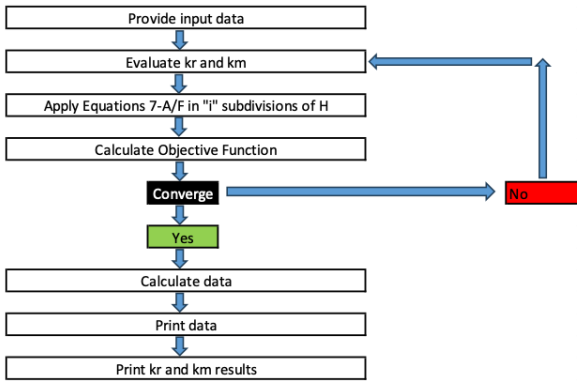

Figure 2. Proposal of a resolution algorithm for k_m and k_r.

This statistical treatment generates the matrix $C_{NH4+cal}$, which must be a three-dimensional matrix of order i×j×k. The index i is related to the pollutant concentration at the lower inlet, j is the sulfuric acid concentration at the upper inlet, and the index k is the column height. However, the surface response only provides a two-dimensional solution i×j on the k=0 plane. Therefore, the solution at height uses regressions of linearized equations, employing the average angular coefficients generated in the experiments. That is, for any k≠0, the regression ln (C_{NH4+}) z is applied. Therefore, there are two statistical treatments: the surface response and the projection of the regressions. The model data are a function of k_m and k_r, and the inlet conditions are represented by the matrix $C_{NH4+cal}$, also of order i×j×k. In this work, mathematical modeling assumed that the reaction has pseudo-first-order kinetics; therefore, the product concentration becomes numerically only a function of the pollutant concentration, and no longer a direct function of the sulfuric acid concentration. This reduces the order of the matrices $C_{NH4+cal}$ and $C_{NH4+exp}$ to i×k, reducing the number of points to be arranged in the matrices; as a consequence, it virtually brings the contribution of the purification solution concentration variable, now hidden, into the constant k_r.

However, the surface response continues to be function of the hidden variable. To address this inconvenience, the solution was used only at the central point for this variable (73.6g/L). For the numerical solution, starting from z=H until z=0 is reached, the concentration points were calculated discretely in each slice of the interval, forming a profile $C_{S,K(z)}$ for each substance S in each phase K. At the top boundary, all conditions are known, in compliance with the boundary conditions described by Equation 11. Since the constants k_m and k_r are not process data, they require an initial estimate (1s-1 were used for both constants) and re-estimate at each iteration: a new matrix $C_{NH4+cal}$ is formed, and the Objective Function of Equation 13 is iteratively recalculated until convergence occurs (Figure 2).

RESULTS AND DISCUSSION

Transient Regime

To experimentally verify whether the column was already in a steady state after 18min, two time-varying tests were performed: T-1 and T-2. Samples were collected from the lowest collection point at different times after starting the timer (step (e) of item 2.2). In both tests, 20mL of ammonium hydroxide (step (b)) and 10mL of sulfuric acid (step (c)) were used. In test T-1, aliquots were collected after 1, 5, and 7min; for T-2, at 2, 6, and 8min. In Figure 3 it is possible to observe that, as expected by the model predictions, a steady state was indeed formed. Subsequently, it was possible to apply linear regressions of the ln (C_{NH4+}) versus t functions to each test individually and evaluate the time required for the exponential curves to reach variations of less than 1% per minute, which is a criterion used to define stability. Table 2 presents the results of the temporal correlations, with a mean response of 8.15 ± 0.76min. Note also the R^2 values above 0.995, indicating an exponential decay suitable for the prediction of a transient model, for which the term $d[C_{NH4+}]/dt$ would be present in the equation. Finally, 18min is a reasonably longer time than that required for system stabilization.

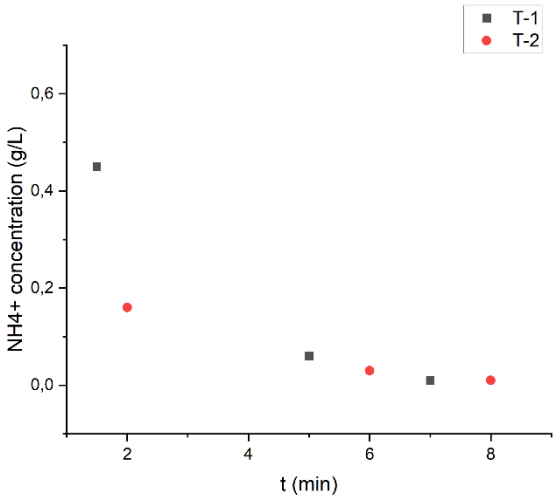

Figure 3. Tests to verify the transient behavior during the first minutes of operation

Table 2. Linear regression of temporal trials

Test	*Angular coefficient*	*Linear coefficient*	R^2	*Stationary Regime time*
T-1	-0,6261	0,1665	0,9983	7,62min
T-2	-0,4114	-1,0290	0,9970	8,69min

Stationary Regime

The tests were performed according to the 3^2 factorial (Table 1), with inlet concentrations calculated

according to Equations 3 and 4, respectively; and samples analysis taken at z=0, z=16, and z=32cm, and the removal percentage for each test was calculated according to Equation 6.

Table 3 presents the results, where it is possible to observe that within the bed fraction analyzed, for the nine tests, there is a removal (y) > 0, and that within each test, there is always a relationship $C_{NH4+,z=0cm} > C_{NH4+,z=16cm} > C_{NH4+,z=32cm}$. This means that within this range of species concentration conditions, the reaction occurs without allowing excess uncaptured pollutants; that is, there is always sufficient acid to drag the pollutant downward.

The ammonium hydroxide concentration in the bottom flask is very low in all tests, and pollutant generation occurs by continuously heating this same solution. If there was no sulfuric acid to treat this demand downward, or if the quantity of this acid was insufficient, the apparatus could be compared to a pilot distillation column. Therefore, it is of utmost importance that the pilot apparatus functions as a chemical scrubber and not as a distillation column, and experimental conditions must be found in which there is sufficient acid to treat this demand. It is possible to easily verify when one or the other occurs, because if there is insufficient acid, the NH_4^+ concentration would increase as the z-axis moves away from the generating source. In the nine tests, a reduction in the response was observed in all of them, indicating that there was sufficient acid.

Table 3. Operating conditions and respective responses

Test	Inlet		Responses			Remotion (y)%
	$C_{H2SO4l,z=H}$ (g/L)	$C_{NH3g,z=0}$ (g/L)	$C_{NH4+,,z=0cm}$ (g/L)	$C_{NH4+,,z=16cm}$ (g/L)	$C_{NH4+,,z=32cm}$ (g/L)	
1	55.2	7.971	0.695	0.378	0.160	8.7%
2	55.2	4.384	0.562	0.371	0.195	12.8%
3	55.2	0.797	0.050	0.028	0.014	6.3%
4	73.6	7.971	1.529	1.135	0.871	19.2%
5	73.6	4.384	0.735	0.475	0.314	16.8%
6	73,6	0.797	0.358	0.261	0.155	44.9%
7	92.0	7.971	2.860	2.195	1.644	35.9%
8	92.0	4.384	1.038	0.650	0.430	23.7%
9	92.0	0.797	0.170	0.107	0.050	21.4%

From Table 3, linear regressions of ln (CNH_4^+) versus z were obtained for each experimental run, which are presented in Figure 4, where all slopes are negative (ranging from −1.7 to −4.6) and all correlation coefficients ($R^2 > 0.97$) confirm an excellent fit to the exponential decay predicted by Equation 9, consistent with the $d[CNH_4^+]/dz$ term. The sharper slopes observed under higher H_2SO_4 concentrations indicate enhanced NH_4^+ formation and consumption rates, whereas flatter slopes at lower acid strengths or higher NH_3 loadings suggest kinetic or mass-transfer limitations. The overall removal efficiencies ranged from 6.3 to 44.9%, increasing slightly with higher acid concentration and decreasing with pollutant load. These values are considerably lower than the ~98% reported by Lebrero et al. (2013) for similar gas–liquid systems, which can be explained by the higher pollutant inlet concentrations and shorter residence times applied in the present study. Comparable behavior was observed by Flagielo et al. (2025), who reported a decrease in SO_2 removal efficiency from 98 to 73% as inlet concentrations increased from 955 to 1340 ppm. Therefore, the lower efficiencies reported here likely reflect mass-transfer and saturation effects under elevated pollutant loads, confirming that system performance is strongly dependent on the balance between gas concentration, liquid acidity, and available reactive capacity. Overall, the good linear correlations obtained validate the proposed model while highlighting the operational constraints that distinguish real systems from idealized laboratory conditions.

Absolutely, there is no relation between process effectiveness and process efficiency under unfavorable conditions. As it was previously demonstrated, for all factorial combinations, there is an exponential fit with good correlation coefficients; rather, it is expected that longer contact time between phases will be required when the demand is very high. This, in an industrial setting, would require designing a column height sufficient to achieve acceptable removal levels.

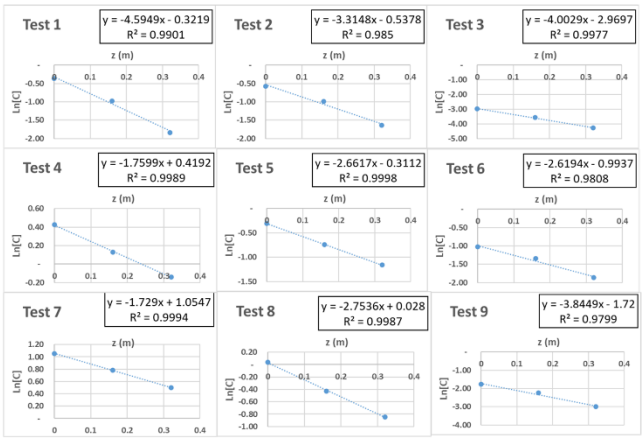

Figure 4. Linear regression ln (C_{NH4+}) *x z* (each test performed) and correlation coefficients

Surface Response

Surface response illustrated in Figure 5 comes from the mathematical expression denoted by Equation 14, whose regression constants values A, B, C and D obtained by STATISTICA 7® software were: A = 0.0219217; B = 0.0028095; C = - 0.0378217 and D = 0.0004583.

$$\frac{(C_{NH4+})_l}{(C_{NH3})_{g,z=0}} = A + B.(C_{H2SO4})_{l,z=H} + C.(C_{NH3})_{g,z=0} + D.(C_{H2SO4})_{l,z=H}.(C_{NH3})_{g,z=0} \quad (14)$$

Figure 5 reveals an increase in removal efficiency as the H_2SO_4 concentration increases. It also shows that for low H_2SO_4 concentrations, the increased demand for the pollutant NH_3 reduces efficiency to lower levels, which may be related to the approach to critical cases where there is insufficient acid for treatment. In these cases, the system pH can reach values > 7.0, where there is chemical equilibrium between the NH_4^+ and NH_3 species, or even migrate to pH values > 10.0, where the NH_3 species is approximately 100% (Behera et al. 2013).

The reduction in efficiency with increasing NH_3 demand occurs up to approximately 80g/L of H_2SO_4 in the purifying liquid composition, and from a value of 85g/L, the contour lines completely inverted, and an increase in efficiency is already noticeable as demand increases. In these cases, a pH below 7.0 is maintained, where the NH_4^+ species predominates. Furthermore, an increase in the concentration of both reactants is expected to significantly slow the reaction rate, a factor that is more important in the case of the acidic species, as it is a two-proton acid in a 2:1 stoichiometric chemical reaction.

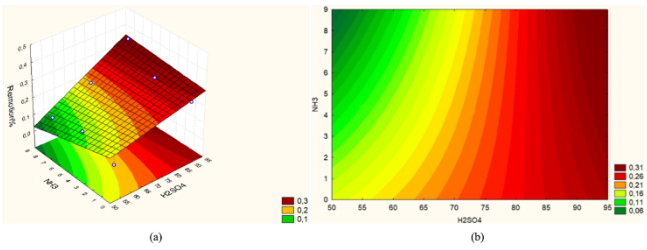

Figure 5. (a) Surface response (b) surface contour

Data regression

After applying the iterative scheme shown in Figure 4, the results k_m = 9.41s^{-1} and k_r = 6.58x$10^4 s^1$ were obtained. Compared with previous studies the same data regression method was applied to a chemical scrubber for chlorine treatment by sodium hydroxide solution, similar result for k_m = 1.037 s^{-1} and a much lower result for k_r = 1.381 s^1 (Soares et. al 2016).

A plausible explanation for the discrepancies between experimental results and simulation predictions lies primarily in the operational conditions and inherent limitations of both the apparatus and the mathematical model. First, the experiments in this work were conducted near the water boiling temperature, whereas the compared studies were performed at room temperature. Despite the higher temperature, the mass transfer magnitude did not significantly increase, likely due to the strong chemical affinity between sulfuric acid and ammonium ions that dominates the system kinetics rather than thermal effects.

The model fits well when sulfuric acid concentration is high and NH_3 demand is low (tests 5, 6, 8, and 9), corresponding to a region of the response surface where the system operates closer to ideal conditions (Figure 6). However, significant deviations appear when acid concentration is low (tests 1, 2, and 3 – Figure 6(a)) or pollutant load is high (tests 4 and 7). These discrepancies can be attributed to two main factors: First, apparatus limitations: the pilot-scale setup relies on a continuous dosing system for NH3, which approximates the actual input but inevitably introduces discontinuities over time. As the pollutant reservoir depletes, the NH_3 concentration fluctuates, particularly at higher demand levels, leading to deviations from the ideal constant concentration assumed in simulations. This effect is evident at tests 1, 4, and 7, where experimental profiles are smoother or less steep than predicted. Moreover, the input pollutant concentration is estimated via Equation 3, based on initial solution volumes rather than direct real-time measurement, increasing uncertainty under high pollutant loads. Second, mathematical model simplifications: the model assumes ideal boundary conditions (Equation 11), where the sulfuric acid concentration at the highest sampling point equals the inlet concentration only if pollutant consumption above that point is negligible. This is an approximation that neglects reactive phenomena occurring between the pollutant source and z=0. As pollutant demand increases, this unaccounted consumption region grows, introducing errors in predicted concentration profiles. Additionally, the model assumes steady-state operation and uniform mixing, disregarding potential hydrodynamic and mass transfer resistances present in the experimental apparatus.

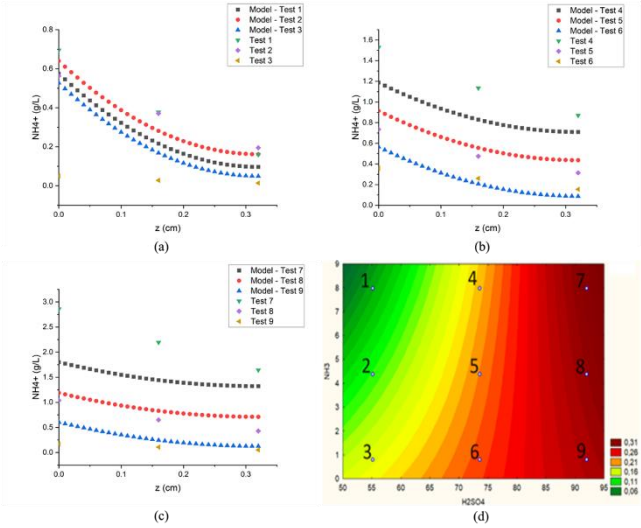

Figure 6. Comparison between experimental data and model prediction: (a) C_{H2SO4} =55.2 g/L – C_{NH3} =7.791g/L (b) C_{H2SO4} =73.6 g/L – C_{NH3} =4.384g/L (c) C_{H2SO4} =92.0 g/L – C_{NH3} =7.791g/L

Finally, test 1 highlights a critical limitation where both reactant concentrations are very low, resulting in the lowest predicted reaction velocity and a significantly smoother experimental decay than the model suggests. This suggests that under conditions near the detection limits or minimal reactive capacity, kinetic parameters and transport phenomena deviate further from idealized assumptions.

In summary, the observed discrepancies between experiments and simulations reflect a combination of pilot-scale apparatus constraints (such as non-ideal dosing and boundary effects) and the inherent simplifications within the mathematical model (idealized boundary conditions and steady-state assumptions). Recognizing these limitations is essential for improving future models and experimental designs to better capture the complex interplay of kinetics and transport in reactive gas-liquid systems.

Simulation

To simulate an industrial case, a device was designed with the same operational conditions as the pilot equipment, for maintaining the information on mass transfer and reaction constants obtained from the model regression. The operation occurs with the following characteristics:

- Industrial steam demand of 27,000m³/h (or 7.43m³/s);
- Purifying solution mass flow rate of 22.3L/min (or 3.71x10^{-4}m³/s);
- Column diameter of 0.6m;
- Pollutant leaving the source at 7.97kg/m³ NH_3;
- Pollutant leaving the treatment below 4.00x10^{-7} kg/m³ NH_3;
- Sulfuric acid concentration of 85g/L

The demand dimensioning corresponds to the production capacity of a local rendering plant, 20t/h of byproduct with 80% moisture, with steam being produced at a specific mass of 0.598kg/m³ from the evaporation and drying water contained in the decomposing meat. The column diameter is estimated to meet the normal velocity of a chimney (between 5 and 7m/s). The flow rate of the purifying solution is 20,000 times lower than the steam flow rate, a ratio close in magnitude to that used in the pilot apparatus operation, which was 3,000 times, but reduced to meet operational criteria. For example, the solution flow rate must be in line with the supply capacity of artesian wells or the municipal network, thus also seeking to minimize the consumption of this natural resource. For the purification solution, it is suggested to use a buffer reservoir of approximately 1.5m³ (which gives the process autonomy for more than 1 hour), in which it can be filled with water and acid is dosed with an appropriate control system. With this liquid flow rate and this diameter, the liquid can pass through the packed column with a spray nozzle at the top. It is recommended to operate with a special centrifugal pump, with components resistant to attack by sulfuric acid, which will be active in the solution; this should be considered when sizing and selecting appropriate materials for the hydraulic system through which the solution will travel. Since this flow rate is approximately the same used in domestic systems (between 12 and 25L/min), connections and piping of the standard domestic size, ¾ or 1inch. The sulfuric acid concentration for the operation was selected according to the acid concentration at which the inversion of the level lines on the response surface was observed. The minimum amount of acid was strategically used within the part of the surface where the model and observations converged, which saves reagent. In addition to the packing, the column is designed with containment devices so it can be operated as a fixed bed. That is, even if the gas velocity reaches the terminal velocity of the packing particles, the fluidization phenomenon will not occur during operation. Finally, a treatment demand corresponding to the simulation concentration in the pilot apparatus was selected, which corresponds to an oversized scenario, or a highly toxic load. For the gas outlet, a reduction of approximately 20 million times below the source and equivalent to 0.4ppm is projected, the minimum value to ensure an acceptable level for human health. However, one of the working conditions that differentiates the experiment from the industrial

environment is temperature. This is because the tests were performed with the pilot column operating at the boiling point of water, 100°C, but in practice, industrial equipment installed in the southern region of Brazil may operate in conditions ranging from colder days, with temperatures close to 0°C, to periods of higher temperatures, which can reach 40°C. According to the literature, the relationship between the reaction rate constant (k_r) and temperature is treated by the Arrhenius Equation and is sometimes approximated as the relationship that increasing the temperature by 10°C causes a twofold increase in the reaction rate constant (k_r). Since the reaction rate is the slowest step in the process, the mass transfer phenomenon will determine how many meters of column will be necessary to ensure sufficient contact time between the phases for the pollutant to disappear from the gas phase. There is indeed a temperature dependence on the equilibrium relationship between the NH_3 and NH_4^+ species (Behera et al. 2013). However, at a temperature of 100°C, ammonia in a neutral solution is expected to be preferably in the gas phase, being negligibly soluble under these conditions. This was also observed experimentally, when the ineffectiveness of the treatment at low acid concentrations was verified. Therefore, it seems reasonable to assume that this mass transfer of such a significant magnitude, even at such an unfavorable temperature for the process, is exclusively caused by a very high affinity of ammonia with the dissolved acid. From this, it is also reasonable to assume that changing the working temperature, in terms of the mass transfer phenomenon, will have a negligible effect compared to changing the pH. However, although a mass transfer magnitude is expected to be independent of temperature, changing the temperature to milder levels directly impacts the chemical reaction rate, as the Arrhenius relationship applies, and it will slow down, requiring more column meters. This is not for the first stage, which would be captured, but for the captured pollutant to be stabilized in the form of ammonium ions (second stage), since, as already mentioned, the first stage depends exclusively on the mass transfer coefficient. To observe this scenario, operations were simulated at 100 and 0°C, varying only the numerical value of k_r (Figure 7)

Figure 7 shows that the model corroborates the expectations discussed. First, regardless of temperature, approximately 3.5m of column is required for the 8g/L of pollutant to reach acceptable levels. Second, the variation in temperature between 0 and 100°C demonstrates that the change will occur in the second part of the mechanism (chemical reaction) and subsequent product form stabilization. This leads us to another important issue: the production of effluent enriched with ammonium sulfate. For a demand of approximately 8g/L in pollutant generation, in a 100% conversion scenario, and considering a 2:1 reaction stoichiometry (or 2x17g:1x132g), it is expected that 31g/L of ammonium sulfate will be produced at the end of the reaction. This reaction will clearly not end within the column, with the reaction being completed in a receiving tank where there will no longer be contact between the phases. Since the solubility of this material is approximately 413g/L at 0°C (13 times higher than generation) (Haynes et al. 2016), there is room for liquid recirculation and consequent savings: in water consumption, sulfuric acid consumption, and finally in the transportation of a more concentrated product for possible buyers. To achieve this, it is possible to install a recycling and purging system in the process and calibrate the inlet flow rates of fresh solution versus the amount being circulated. This process must consider the actual industrial process demand, including production fluctuations and consequent mass transfer constant reduction with the solution's saturation process.

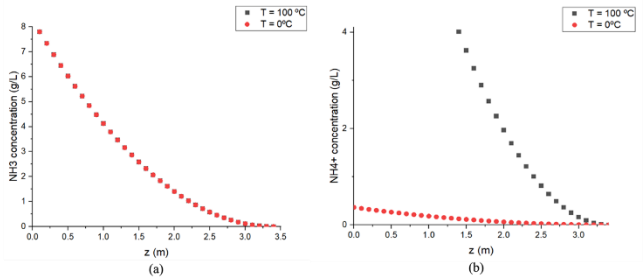

Figure 7. Industrial column simulation operating with 85g/L of sulfuric acid and responses for the concentration of NH_3 and NH_4^+ along the column under different temperature conditions

CONCLUSION

In this study a coupled experimental and numerical investigation was conducted in a pilot-scale chemical scrubber; tests were performed at three different concentrations of ammonia and sulfuric acid. The results showed that the apparatus can observe the formation of a steady state, and the adopted methodology allowed for the collection of results at different reagent concentration levels at the equipment inlets, which facilitated the observation of variations in treatment efficiency.

The experimental procedure developed generated information (database) that, after statistical analysis, demonstrated high efficacy provided sufficient acid was available, and that this parameter was the most effective in removing the pollutant. The mathematical model was suitable for a significant portion of the response surface. Industrial scenarios, considering the

effect of operating temperature, revealed that it is possible to treat the pollutant with appropriately sized equipment under selected conditions, while simultaneously following strategies that provide greater savings and, ultimately, provide environmentally safe disposal of the product generated, enabling the scale-up of a project that has proven viable and sustainable.

Furthermore, the study is enriched by the fact that data collection at different points along the axial axis allows for the observation of the formation of exponential profiles resembling those predicted by classical phenomenological models of Chemical Engineering. The proposal of a numerical solution also allowed for further inferences regarding the conditions under which the apparatus deviates from the idealities predicted by the model. Thus, observations from nature are combined with the classical mathematical approaches

REFERENCES

Abdi, M.; Alinezhad, E.; Sene, R.; Haghighi, M.; Keshizadeh, H. (2020) Evaluation of a pilot-scale scrubber for the mitigation of NH3 emissions from laboratory animal houses in the presence of different oxidants. Journal of Environmental Chemical Engineering, Vol. 8, 10378. DOI: https://doi.org/10.1016/j.jece.2020.103708.

Alinezhad, E.; Haghighi, M.; Rahmani, F.; Keshizadeh, H.; Abdi, M. (2019) Technical and economic investigation of chemical scrubber and biofiltration in removal of H2S and NH3 from wastewater treatment plant. Journal of Environmental Management, v. 241, p. 32-43, DOI: https://doi.org/10.1016/j.jenvman.2019.04.003.

Barros Neto, B. et al. (2001) Como fazer experimentos - pesquisa e desenvolvimento na ciência e na indústria. 2. ed. Unicamp.

Behera, S.N.; Sharma, M.; Aneja, V.P.; Balasubramanian, R. (2013) Ammonia in atmosphere: a review on emission sources, atmospheric chemistry and deposition on terrestrial bodies. Environmental Science and Pollution Research, v. 20, p. 8092-8131. DOI: https://doi.org/10.1007/s11356-013-2051-9.

Flagiello, D.; di Natale, F,; Sebastiani, I.; Nava, F.; Milicia, A.; Lancia, A.; Erto, A. (2025). Experimental and modelling study of ammonia-based FGD scrubbers. Chemical Engineering Science, v. 305, 121101. DOI: https://doi.org/10.1016/j.ces.2024.121101.

Fthenakis, V.M. (2001) Water-spray systems for mitigating accidental indoor releases of water-soluble gases. Journal of Loss Prevention in the Process Industry, v. 14, n. 3, p. 205-211. DOI: https://doi.org/10.1016/S0950-4230(00)00025-5.

Haynes, W.M. et al. (2016) Handbook of chemistry and physics: a ready-reference book of chemical and physical data. 97. ed. Boca Raton, p 5:17.

Kjeldahl, J. (1883) A New Method for the Determination of Nitrogen in Organic Matter. Zeitschrift für Analytische Chemie, 22, 366-382. http://dx.doi.org/10.1007/BF01338151.

Lebrero, R.; Rangel, M.G. L.; Muñoz, R. (2013) Characterization and biofiltration of a real odors emission from wastewater treatment plant sludge. Journal of Environmental Management, v. 116, p. 50-57. DOI: https://doi.org/10.1016/j.jenvman.2012.11.038.

Prostejovsky, T.; Spácilová, L.; Reli, M.; Zebrák, R,; Kocí, K. (2025) Highly effective technology for ammonia abatement from industry operations. Separation and Purification Techonology, v. 376, 134017. DOI: https://doi.org/10.1016/j.seppur.2025.134017.

Soares, C.; Bastos, J. C. S. C.; Wiggers, V. R.; Decker, R. K.; Noriler, D.; Meier, H. F. (2016) Experimental and numerical investigation of a reactive absorption column for chlorine gas mitigation. Chemical Engineering Communications, v. 203, n. 7, p. 924-932. DOI: https://doi.org/10.1080/00986445.2015.1126582.

Yildirim, O.; Kiss, A. A.; Huser, N.; Lessmann, K.; Kenig, E. Y. (2012) Reactive absorption in chemical process industry: a review on current activities. Chemical Engineering Journal, v. 213, p. 371-391. DOI: https://doi.org/10.1016/j.cej.2012.09.121.

To cite this paper, use:

Moser, V.M., Silva, M.K. & Bastos, J.C.S.C. (2025). Ammonia Gas Mitigation by Reactive Absorption. *Multi-Science Journal*, 8(1): 42-51. DOI: *https://doi.org/10.33837/msj.v8i1.1738*